Structure of Two Subfractions of Normal Porcine (*Sus domesticus*) Serum Low-Density Lipoproteins. X-ray Small-Angle Scattering Studies†

Günther Jürgens, Gabriele M. J. Knipping, Peter Zipper, Renata Kayushina, Gábor Degovics, and Peter Laggner*

ABSTRACT: Two subfractions of low-density lipoproteins (LDL) were isolated from normal pig (*Sus domesticus*) serum by a combined method including precipitation, ultracentrifugation, and gel chromatography. The fractions recovered from the buoyant density ranges 1.020–1.050 and 1.050–1.090 g/mL, denoted as LDL_1 and LDL_2, respectively, were studied with regard to structure and thermotropic behavior by X-ray small-angle scattering and were compared to human serum low-density lipoprotein of density 1.020–1.063 g/mL. The average molecular weights determined from the scattering intensities on an absolute scale were 2.6×10^6 and 2.0×10^6 for LDL_1 and LDL_2, respectively. The maximum particle diameters were found to be 24 and 21 nm, respectively. Both species were found to have quasi-spherical symmetry and to display the thermotropic transition of the apolar lipids within the particle core similar to human LDL. The width of the transition was approximately 9 °C in both cases, but the midpoint transition temperature was higher by 8 °C for LDL_1 (33 °C) than for LDL_2 (25 °C). Despite their different sizes and thermotropic behavior, the two porcine LDL subfractions appear to be built according to the same structural principle as human LDL in the molecular organization of the apolar lipids within the particle core.

Since the pioneering studies of Gofman et al. (1954), numerous studies have contributed to evidence of the important role of low-density lipoproteins (LDL)[1] in the development of atherosclerotic diseases (Jackson & Gotto, 1976; Eisenberg, 1976; Fisher, 1976; Goldstein & Brown, 1977). However, the elucidation of metabolic events at the level of molecular structure is still largely incomplete. In investigations on lipoprotein metabolism and on the pathobiochemistry of atherosclerosis, animals have frequently been used for model studies. A widely used species has been the pig (*Sus domesticus*). Thus, Janado et al. (Janado et al., 1966; Janado & Martin, 1968) first made the observation that porcine serum obtained from normolipemic animals contains two distinct fractions of low-density lipoproteins differing in modal buoyant density, molecular weight, and particle size (Calvert & Scott, 1975). These two subfractions, termed LDL_1 and LDL_2, were found to be identical in their apolipoprotein composition (Jackson et al., 1976) and to be very similar to human LDL (Knipping et al., 1975). Thus, porcine LDL offers a highly favorable system for investigations of the microheterogeneity of LDL, which has also been found to exist, although to a different extent, in normal and hyperlipidemic man (Fisher et al., 1972; Lee, 1976). Previous X-ray small-angle scattering data on the structure of human LDL (Laggner et al., 1976; Tardieu et al., 1976; Atkinson et al., 1977; Müller et al., 1978) resulted in the postulation of structural models for the molecular architecture of LDL. A similarly detailed investigation on the two LDL subfractions of normolipemic porcine serum is still lacking. The present study has been undertaken to fill this gap and to compare the structural data from X-ray small-angle scattering of differently sized LDL species, as provided by the two porcine LDL subfractions, with the corresponding data on human LDL. This should provide further insight into the structural variability within the normal LDL density range. We also investigated the detailed temperature course of the thermotropic order–disorder transition of the apolar lipids within the two subfractions since it is likely that, among other variables, molecular size may also have a distinct effect on the thermal behavior of LDL particles. This is of particular interest since it has been proposed (Deckelbaum et al., 1975; Laggner et al., 1977; Laggner & Kostner, 1978) that the physical state of the lipids within the particles may be of relevance to the metabolic fate of LDL and consequently to the development of atherosclerosis.

Experimental Procedures

Preparation of Serum Lipoproteins. Pig serum was collected from normal house swine (*Sus domesticus*) after overnight fasting. For the preparation of human LDL fresh plasma was obtained from several healthy donors. Preparation of pig and human LDL was carried out in essentially the same way. After the addition of NaN_3 (1 mg/mL) and ethylenediaminetetraacetic acid (disodium salt; 0.1 mg/mL) to the pig serum, LDL and VLDL were precipitated with sodium phosphotungstate and $MgCl_2$ (Burstein & Morfin, 1969). The precipitate was separated and subsequently solubilized by addition of sodium citrate and dialyzed against 0.15 M NaCl. A density of 1.020 g/mL was adjusted by addition of NaBr. After the solution was spun in a preparative ultracentrifuge (Sorvall ODT2) at 120000*g* for 22 h, LDL was separated from the VLDL floating on the top of the tube. The density of the material in the lower third of the tube was then increased to 1.050 g/mL and the material was centrifuged at 140000*g* for 22 h. The floating material representing LDL_1 was removed. The density of the sediment was then adjusted to 1.090 g/mL, and the material was centrifuged as described above. The material in the upper fourth of the tube containing LDL_2 was collected. In addition, the two density fractions were recentrifuged at the densities mentioned above. For further puri-

† From the Institut für Röntgenfeinstrukturforschung der Österreichischen Akademie der Wissenschaften und des Forschungszentrums Graz, Steyrergasse 17, A-8010 Graz, Austria (P.L. and G.D.), the Institut für Medizinische Biochemie der Universität Graz, Graz, Austria (G.J. and G.M.J.K.), and the Institut für Physikalische Chemie der Universität Graz, Graz, Austria (P.Z.). *Received July 21, 1980.* R.K. was a visiting scientist from the Institute of Crystallography of the Academy of Sciences of the USSR, Moscow. This work was supported by the Österreichischer Fonds zur Förderung der Wissenschaftlichen Forschung under projects 3524 (P.L.) and 2836 (A.H.).

[1] Abbreviations used: LDL, low-density lipoprotein; LDL_1, buoyant density fraction 1.020–1.050 g/mL; LDL_2, buoyant density fraction 1.050–1.090 g/mL; VLDL, very low density lipoprotein.

0006-2960/81/0420-3231$01.25/0

fication, the LDL fractions were chromatographed over a Bio-Gel A5m (Bio-Rad Laboratories) (100 × 2.5 cm) column in 0.1 M Tris-HCl buffer, pH 7.5. Human LDL were prepared in a density region of 1.020–1.063 g/mL.

The LDL fractions were tested with antisera against HDL to check their purity. Human LDL was additionally tested for contamination with Lp(a) (Jürgens & Kostner, 1975). Electrophoresis was carried out on 0.5% agarose gels and on 3% and 10% polyacrylamide gels (Kostner & Holasek, 1972; Frings et al., 1971). Delipidation of the lipoproteins was performed as described previously (Jürgens & Kostner, 1975). Determination of total and esterified cholesterol was performed with a test kit supplied by Merck (Merckotest, cholesterol enzymatic, no. 14350). Triglycerides were estimated by using a test combination by Boehringer Mannheim (no. 15940). Phospholipids were determined according to Bartlett (1959), and protein concentrations were measured according to the method of Lowry et al. (1951) with 0.1% sodium dodecyl sulfate in the reaction mixture and bovine serum albumin as a standard. Before the measurements, the LDL samples were checked by sedimentation or flotation runs in the analytical ultracentrifuge (Beckman Model E).

X-ray Small-Angle Scattering. In the present study a recently described modification, the "integrated camera" (Stabinger & Kratky, 1979), of the conventional block collimation system (Kratky, 1954) has been used to measure the X-ray small-angle scattering curves. The advantage of the integrated camera over the previous type lies in its considerably higher efficiency in the use of the radiation source and in its lower background scattering level. This allows high-quality scattering data within short exposure times to be obtained by using the line focus of a sealed X-ray tube (Cu anode) powered to 1.4 kW by a conventional stabilized generator (Philips PW 1730). The scattering curves were recorded within an angular range of $7 \times 10^{-2} < h < 2.86$ nm^{-1} ($h = (4\pi \sin \theta)/\lambda$; 2θ scattering angle; $\lambda = 0.154$ nm, Cu Kα wavelength) at intervals of $\Delta h = 1 \times 10^{-2}$ nm^{-1} for $h < 0.2$ nm^{-1}, and $\Delta h = 4.08 \times 10^{-2}$ nm^{-1} for $h > 0.2$ nm^{-1}. Six subsequent angular scans with a minimum of 6×10^4 pulses accumulated at each point were performed for each sample and for the blank exposure. The highest concentration (~40 mg/mL) was used to measure the entire scattering curve, and serial dilutions were studied to eliminate the concentration effect in the lowest angular region ($h < 0.4$ nm^{-1}). The exposure times for any single sample did not exceed 5 h. After blank subtraction and statistical evaluation (Zipper, 1972), the scattering data were corrected for the geometrical collimation error (Kratky et al., 1960) and for the influence of the Cu Kβ line not discriminated by the proportional counter (Zipper, 1969) by a computer program developed by Glatter (1977a) on the Univac 1100/80 computer of the Rechenzentrum Graz. For molecular weight determinations the primary beam intensity was measured with the recently described moving slit accessory (Stabinger & Kratky, 1978).

Specific Volume Determination. The densities of lipoprotein solutions and of the dialysis equilibrium buffer were measured to an accuracy of seven decimal digits by the hollow oscillator method (Kratky et al., 1973) with a DMA 60 density meter with two external measuring cells DMA 602 (Anton Paar, Graz, Austria) thermally coupled in a thermostat circuit operating in the reference mode (Laggner & Stabinger, 1976). When the reference cell is filled with equilibrium buffer, or any other aqueous solution with a similar thermal expansion coefficient, and its oscillation period is used as the time base for the sample cell, the disturbing influence of minor temperature variations is practically abolished, and thus the precision of the oscillator principle can be fully realized.

Table I: Chemical Composition of Porcine LDL Subfractions and of Human LDL[a]

	LDL	porcine	
	LDL (d 1.020–1.063 g/mL)	LDL_1 (d 1.02–1.05 g/mL)	LDL_2 (1.05–1.09 g/mL)
protein	21.8 ± 1.0	27.9 ± 1.4	32.4 ± 0.9
phospholipid	22.0 ± 1.2	22.4 ± 2.0	22.5 ± 1.0
cholesterol	10.3 ± 2.5	10.4 ± 2.2	9.9 ± 0.6
cholesteryl esters	40.3 ± 2.6	37.0 ± 2.7	31.6 ± 1.4
triglycerides	5.6 ± 1.4	2.3 ± 0.5	3.6 ± 0.7

[a] Values are given in weight percent ± standard deviation from three separate analyses.

Apparent specific volumes of the lipoprotein fractions were calculated from the density difference Δd between LDL solutions and the equilibrium dialysis buffer according to

$$\phi_2' = \frac{1}{d_{\text{buffer}}}(1 - \Delta d/c) \quad (1)$$

where c is the lipoprotein concentration in grams per milliliter. No concentration dependence of ϕ_2' could be observed at concentrations below 20 mg/mL. At the low salt concentration used in the present studies, the redistribution of low molecular weight components between the solvent and solution compartments at dialysis equilibrium can be safely neglected for the purpose of the calculation of electron densities and molecular weights.

Results

Chemical Analysis. The chemical compositions of the porcine LDL subfractions and of human LDL are listed in Table I. In both fractions the protein content was found to be considerably higher than in human LDL whereas the triglyceride content was significantly lower. In agreement with its higher buoyant density, LDL_2 was found to have a higher protein and correspondingly lower cholesteryl ester content. These results are within the range of most of the previous records found in the literature (Janado & Martin, 1968; Fidge & Smith, 1975; Calvert & Scott, 1975), while the protein values reported by Jackson et al. (1976) are considerably lower. The electrophoretic mobility in 3% polyacrylamide gels was found to be higher for LDL_2 than for LDL_1. This is in agreement with the higher protein content and smaller particle size of the LDL_2 fraction.

Specific Volumes and Molecular Weights. The apparent specific volumes and the molecular weights determined from the absolute scattering intensity at zero angle (Kratky et al., 1951; Kratky, 1963) are listed in Table II. These results are in agreement with the values found by ultracentrifugation by Janado et al. (1966). Table II also includes the theoretical radii of unhydrated equivalent spheres consistent with the experimentally found values for M_r and ϕ_2'. These theoretical values are of interest in the following discussion of shape anisotropy and solvation.

Particle Size, Shape, and Internal Structure. The X-ray small-angle scattering curves of the two subfractions of porcine LDL show qualitatively very similar characteristics to those of human LDL (Figure 1). The well-defined secondary maxima indicate that, similar to human LDL, the porcine LDL subfractions are isometric, spherelike structures with internal electron density fluctuations (Laggner & Müller, 1978). Minor differences between the different samples appear in the sharpness of the maxima and minima. LDL_2 and human LDL

Table II: Specific Volumes and Molecular Weights of Porcine LDL Subfractions

	ϕ_2' (mL/g)[a]			r_0 (nm)[c]	
	4 °C	37 °C	$M_r \times 10^{-6}$ [b]	4 °C	37 °C
LDL_1 (*d* 1.020–1.050 g/mL)	0.939 ± 0.003	0.965 ± 0.002	2.6 ± 0.3	9.9	10.0
LDL_2 (*d* 1.050–1.090 g/mL)	0.920 ± 0.003	0.943 ± 0.003	2.0 ± 0.2	9.0	9.1

[a] Apparent specific volume at dialysis equilibrium (isopotential specific volume). Mean ± SD from triplicate determinations. [b] Weight-average molecular weight determined from the absolute scattering intensity at zero angle. For estimating the errors, the individual errors in the measurements of absolute intensity, specific volume, and concentration were taken into account. [c] Radii of equivalent unsolvated spheres calculated from $r_0 = [(3.966 \times 10^{-4}) M\phi_2']^{1/3}$.

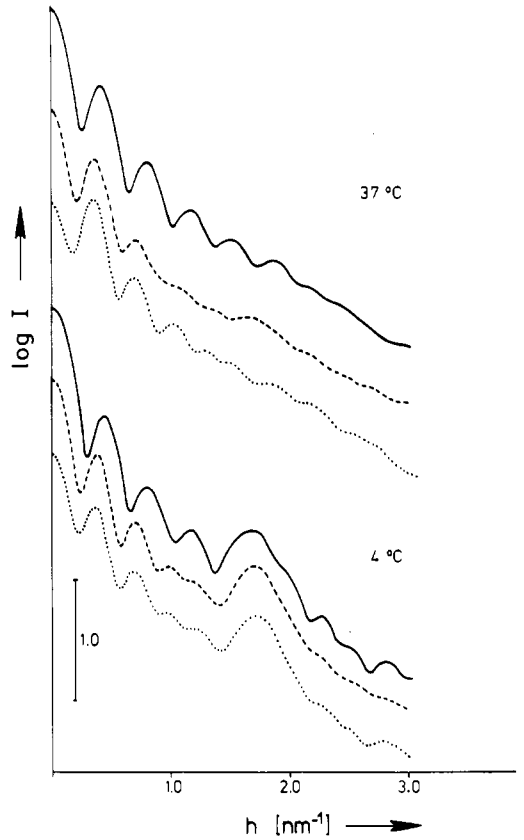

FIGURE 1: X-ray small-angle scattering curves, corrected for collimation error, of porcine LDL_1 (---), porcine LDL_2 (—), and human LDL (···) at 37 (top three curves) and 4 °C (bottom three curves).

show slightly sharper maxima than LDL_1, particularly at 37 °C. Porcine LDL of the same density cut as used in human LDL (1020–1063 g/mL) show a stronger smearing of the scattering pattern than human LDL (results not shown), probably due to a higher degree of polydispersity. The angular positions of the maxima of LDL_2 are shifted progressively to larger angles as compared to LDL_1 or human LDL, indicating a smaller particle size for LDL_2. An exception to this behavior is made by the intense maximum of $h = 1.7$ nm^{-1} at 4 °C which occurs at identical positions with all three samples. Similar to human LDL, the two porcine LDL fractions show a strong temperature dependence on the $h = 1.7$ nm^{-1} maximum.

More direct and quantitative structural information is obtained from the Fourier transforms of the scattering curves, the electron-pair distance distribution function $p(r)$ (Figure 2) being obtained from the scattering curves $I(h)$ according to eq 2.

$$p(r) = (2\pi^2)^{-1} \int_0^\infty I(h) hr \sin hr \, dh \qquad (2)$$

In the present work the $p(r)$ functions were obtained in parallel to the desmeared scattering curves $I(h)$ by the method

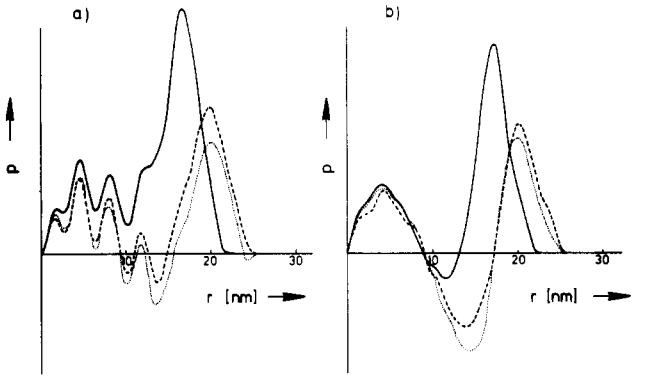

FIGURE 2: Pair distance distribution functions $p(r)$ of porcine LDL_1 (---), porcine LDL_2 (—), and human LDL (···) at 4 (a) and 37 °C (b).

of indirect Fourier transformation of the uncorrected experimental scattering curves (Glatter, 1977a). The optimal choice of the maximum value of r, where $p(r) \neq 0$, was found by searching for the optimally stabilized solution; r_{max} values of 23 nm for LDL_1 and 26 nm for LDL_2 and human LDL were thus obtained. The numbers of auxiliary Spline functions used to form the $p(r)$ functions in Figure 2 were 22 for LDL_1 and 25 for LDL_2 and human LDL, respectively. Tests with higher values of r_{max} produced unspecific minor oscillations about $p(r) = 0$ at $r > 23$ and > 25 nm, respectively.

The $p(r)$ functions, which are statistics of all distances between any two electrons within one particle, provide as an immediate result an estimate of the maximum particle diameter, i.e., the distance r where $p(r)$ becomes zero. Thus, diameters of 24 (25) and 21 (22) nm, for porcine LDL_1 and LDL_2 (figures in parentheses are the corresponding values at 37 °C) are obtained at 4 °C. For comparison, the human LDL sample of the present study yielded a diameter of 24 (25) nm. Combining these results with the theoretical diameters of spheres with volumes corresponding to the respective molecular weights and specific volumes (Table II) indicates frictional ratios of 1.22 and 1.18 for LDL_1 and LDL_2, respectively. It is important to note, however, that this calculation of frictional ratios is only correct for compact, unsolvated model bodies with ideal size and shape homogenety. Moreover, it should not be overlooked that the material isolated in discrete buoyant density fractions is still likely to be heterogeneous. Since the $p(r)$ function provides the maximum diameter of the largest particles, while the molecular weights and specific volumes are average values, it is clear that such a situation would also mimic shape anisotropy, even with an assembly of ideal spheres. On the other hand, the calculation of model scattering curves has shown, for example, that ellipsoids of revolution with the above frictional ratios fail to produce scattering curves with such pronounced side maxima as obtained from the present LDL fractions. It is, therefore, evident that the above calculation of frictional ratios leads to an overestimation of shape anisotropy and that the particles are considerably closer to spherical.

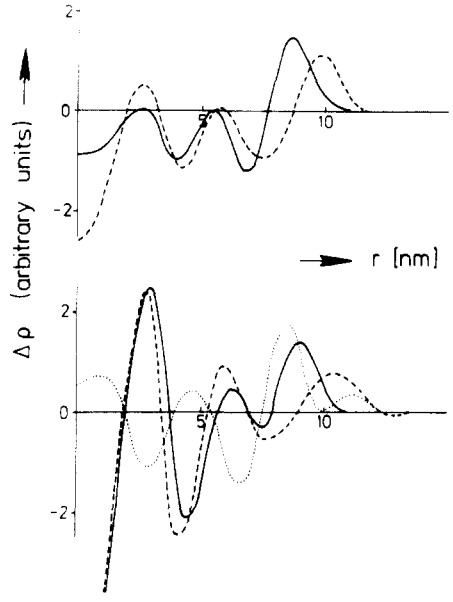

FIGURE 3: Radial electron density contrast distributions of porcine LDL_1 (---) and LDL_2 (—). Top frame, 37 °C; bottom frame, 4 °C. The dotted line at 4 °C was obtained by using an amplitude phase assignment of + − + − + for the first five maxima.

Apart from the particle size, the $p(r)$ function provides some important direct information about the internal particle structure. At 4 °C both porcine LDL_1 and LDL_2 show the same high frequency of electron pairs regularly spaced at odd multiples of approximately 1.7 nm at distances smaller than 15 nm. Remaining traces of this regularity are also shown at 37 °C by LDL_1 while in LDL_2 and in human LDL these ripples are essentially absent at this temperature. From this it is evident that the inner structure of the two LDL subfractions, despite their different particle sizes, contains at low temperatures the same ordered arrangement of molecular constituents which is also present in human LDL. Extensive model studies similar to those described in a previous report on lipoprotein B from human LDL (Müller et al., 1978) have shown that the observed sharpness and regularity of these maxima in the $p(r)$ functions at 4 °C are consistent with the assumption of a spherically symmetric repeat as the basis of this ordered arrangement.

Since it is evident from all these considerations that spherical symmetry, at least at low resolution, is consistent with the experimental results and thus provides a valid approximation to the particle structure (see Discussion), the scattering curves were further analyzed by Fourier transformation of the amplitudes $F(h) = \pm[I(h)^{1/2}]$ by use of the previously described method of extrapolation to zero of the experimental minima (Laggner et al., 1976). Thus, by use of eq 3 the radial electron

$$\Delta\rho(r) = (2\pi^2)^{-1}\int_0^\infty F(h)h^2\frac{\sin(hr)}{hr}\,dh \qquad (3)$$

density distribution $\Delta\rho(r)$ is obtained (Figure 3). For this computation the numerical least-squares approximation method of indirect Fourier transformation (Glatter, 1977b) was used to minimize the curve termination error. The calculation included the scattering data up to a maximum angle of h = 2.0 nm^{-1}. The assignment of the phases was the same (+ − + − + −) as previously used (Laggner et al., 1976, 1977; Müller et al., 1978) for lipoprotein B from human LDL except for LDL_2 at 4 °C, where a phase sequence + − + − − has been used; i.e., the maximum at h = 1.7 nm^{-1} has been given a negative sign in all cases. To demonstrate the effect of the alternative phase sequence, + − + − +, its resulting electron density profile is also depicted in Figure 3.

This choice of phases, + − + − −, is supported by an alternative approach to obtain the radial electron density distribution involving the direct, three-dimensional deconvolution of the distance distribution function $p(r)$ by a numerical method.[2] While this approach (Figure 4) invariably leads to zero minima between the first six maxima for LDL_1, it reproduces the third and fourth side maxima of LDL_2 at 4 °C as a double maximum, i.e., not separated by a zero minimum where the phases could change sign, thus leading to a negative sign for the h = 1.7 nm^{-1} maximum.

Thermotropic Behavior. As already suggested by the above scattering data at 4 and 37 °C, the two porcine LDL subfractions show a similar but not quantitatively identical temperature behavior. To study the temperature course of the thermal transition more closely, the maximum in the scattering curves at h = 1.7 nm^{-1} was measured at temperature intervals of 5 °C and the peak heights were plotted as a function of temperature (Figure 5). This experiment revealed a difference of about 8 °C in the transition temperature, defined by the temperature of the steepest slope in Figure 5, which is about 33 °C for LDL_1 and 25 °C for LDL_2. With 30 min for equilibration at each temperature there was no noticeable hysteresis. With time intervals of 15 min and less, a 1–2 °C hysteresis was observed; however, it is difficult to ascribe this effect unambigously to the sample, due to uncertainties with regard to the heat flow in the entire Peltier cuvette assembly. For comparison, several human LDL samples were tested in the same manner and showed midpoint transition temperatures between 22 and 34 °C [see also Deckelbaum et al. (1977)].

Discussion

In describing the heterogeneity of LDL, several aspects such as buoyant density, particle size, molecular weight, chemical composition, and antigenic determinants have to be taken into account. Quite clearly, heterogeneity with respect to any single one of these parameters must have its expression also in details of the molecular structure. It is the aim of the present study to achieve a better insight into this structural heterogeneity of LDL.

By the classification "low density", only lipoproteins in the density range 1.006–1.063 g/mL should be considered. Nevertheless, lipoproteins isolated from a higher density range are frequently also designated as low-density lipoproteins. Albers et al. (1972) described a human serum lipoprotein which could be prepared in the flotation range of S_f 0–2. It was identified immunochemically and electrophoretically as a species belonging to LDL and termed as LDL_3. For its molecular weight, a value of 1.8×10^6 was determined. As discussed by Calvert & Scott (1975), this human LDL_3 should be homologous to the porcine LDL_2 subfraction. Indeed this fraction is found to much higher concentrations in the pig than in humans, where only traces of LDL_3 could be detected. On

[2] This deconvolution square root technique (Glatter, 1980) allows the computation of the electron-density distribution from the distance distribution function $p(r)$ in the case of approximately spherically symmetric particles. The electron-density profile $\rho(r)$ is approximated by a linear combination of equidistant step functions $\rho(r) = \sum c_i\varphi_i(r)$. This allows the analytical evaluation of the three-dimensional overlap integral. The system of equations combining the unknown coefficients c_i and the input data $p(r)$ is nonlinear; however, it can be solved by using an iterative weighted least-squares procedure after linearization. It is important to stress that this method is, at present, the only practicable alternative to the use of eq 3 for the evaluation of radial electron density profiles and has the advantage of avoiding the phase problem.

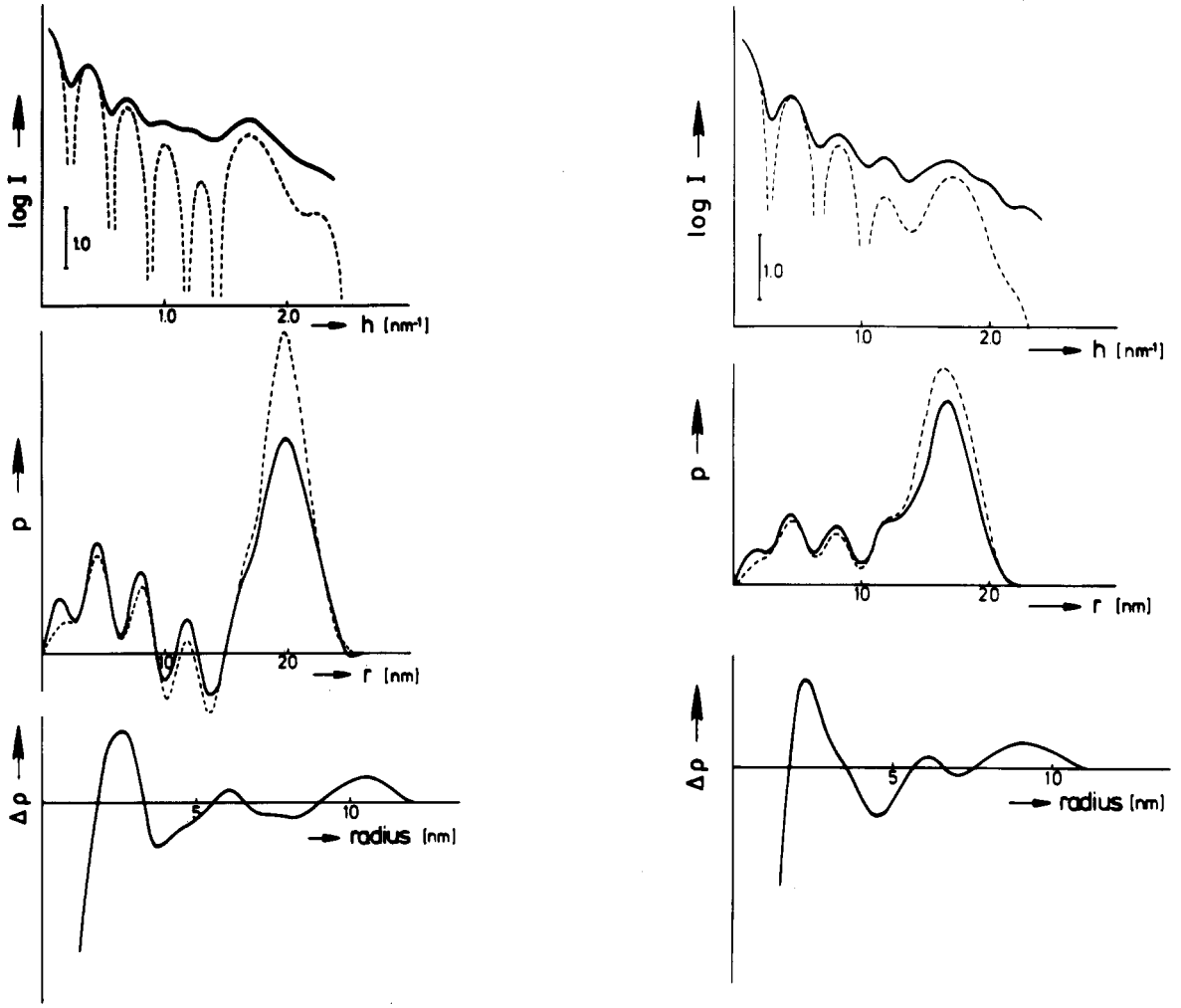

FIGURE 4: Deconvolution of the pair distance distribution functions $p(r)$ for porcine LDL_1 (a, left) and LDL_2 (b, right). Top and middle frames show the experimental (—) and approximated (---) scattering functions $I(h)$ and distance distribution functions $p(r)$, respectively. Bottom frames show the resulting radial electron-density contrast distributions. The smooth lines connect the central plateau heights of the equidistant step functions of 0.65 nm width used in the interative approximation (see footnote 2).

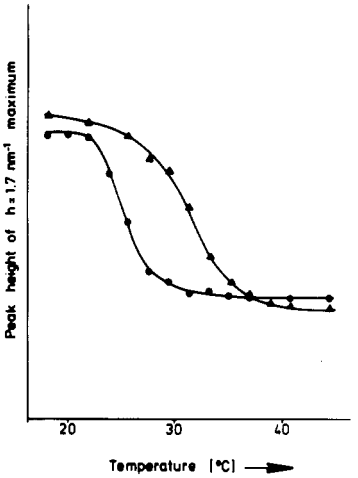

FIGURE 5: Temperature dependence of the intensity of the $h = 1.7$ nm^{-1} maximum of porcine LDL_1 (▲) and LDL_2 (●). The ordinate scale is in arbitrary units.

the other hand, Kostner (1972) described a lipoprotein as LpB_{HDL} which was isolated by immunoadsorption from a fraction of the density range of HDL_1 (1.063–1.090 g/mL). In the intact particle as well as after delipidation no apolipoprotein other than apoB was identified. Because of the high protein content (41%) and the hydrated density of 1.084 g/mL, this fraction was defined as a high-density lipoprotein.

The porcine LDL_2 fraction described in the present work has a protein content of 32%, which is markedly higher than that of porcine LDL_1 or human LDL. Several criteria justify its operational inclusion into the LDL class despite its higher buoyant density: Immunochemically it shows a positive reaction only with anti-B-serum; after delipidation, only traces of apolipoprotein A and C can be detected; both, in agarose gel and polyacrylamide gel electrophoresis, LDL_2 move as one single band with fast β mobility. Perhaps the strongest argument, however, is presented by the characteristic similarity in its X-ray scattering pattern, and hence its molecular architecture, to normal LDL of the density range 1.020–1.063 g/mL.

Both LDL_1 and LDL_2, as shown by the present work, are in first approximation spherical particles. A more detailed shape analysis would require quantitative data on the degree of structural heterogeneity. There is no evidence for the assumption that the present two density fractions are ideally monodisperse solutions. On the other hand, it is likely that any preparation of LDL solely based upon buoyant density fractionation yields a mixture of particles differing to some extent in molecular size and chemical composition. This may reflect the fact that LDL is not a particle species exclusively produced according to strict genetic determination but rather a reaction product of a multiple equilibrium catabolic process. A further inhibitory obstacle to the structural description is given by the well-documented mobility of the molecular con-

stituents of LDL. Therefore, the possibility that the entire particle undergoes time-dependent deformations about an average structure cannot be excluded.

For both above reasons a quantitative analysis of the molecular shape and internal structure, which formally would be feasible by the contrast variation approach (Stuhrmann & Kirste, 1965; Luzzati et al., 1976), is certainly problematic. On the other hand, previous evidence (Müller et al., 1978) has shown that the lipoprotein B from human LDL, which in its scattering behavior is closely similar to the present LDL_1 fraction, has an anisotropy factor of less than 1.05. Since LDL_2 shows even sharper minima and maxima, it is clear that the spherical approximation holds even better in this case.

With respect to the internal structure of the particles, the present study shows that the two LDL fractions have similar patterns of molecular organization. Following the initial postulation by Deckelbaum et al. (1975) and our previous line of argument (Laggner et al., 1976, 1977; Müller et al., 1978, Laggner & Müller, 1978), the particles consist of a core containing the apolar lipids, cholesteryl esters, and triglycerides, surrounded by a monolayer of polar constituents, protein, phospholipid, and cholesterol. At low temperature the apolar lipid core is in an ordered arrangement, most probably consisting of two concentric layers of radially aligned molecules, which undergo a transition to a more disordered structural state within a characteristic temperature range. Deckelbaum et al. (1976) have shown that in human LDL taken from different individuals a weak but significant correlation exists between this transition temperature and the triglyceride/cholesterol ester ratio. According to this correlation the present chemical data (Tabel I) would predict transition temperatures of 30.3 and 27.9 °C. Thus it is likely that the observed difference of 8 °C between the transition temperature of the present two porcine LDL fractions is also influenced by other factors. A possible cause for this effect may lie in the smaller particle size of LDL_2 and its consequently lower absolute number of cholesteryl ester molecules per particle, hence lower cooperativity and increased border effects. A similar dependence of the transition temperature on the particle size has been found in a recent study on LDL from cholesterol-fed *Macaca fascientaris* (Tall et al., 1978). As shown by Pownall et al. (1980), the fatty acid composition of the apolar lipids may be another possible factor in determining the thermotropic behavior. Clearly, for a final decision, a systematic study on the correlations between all these different factors and the characteristics of the transition has to be performed. In any case, it is evident that porcine LDL is heterogeneous not only with respect to particle size but also in the transition temperature of the individual particles.

In conclusion, the present study shows that porcine LDL contains particles of diameters ranging from 21 to 24 nm which are built according to one general structural principle similar to human LDL in which a core of cholesteryl esters and triglycerides is surrounded by a monolayer of polar lipids, i.e., phospholipids and unesterified cholesterol, and protein. This size heterogeneity goes along with strong differences in the thermotropic transition temperature. Since it has been shown that the transition also affects the molecular structure of the surface layer (Laggner & Kostner, 1978), it is tempting to speculate that porcine LDL, of which a considerable fraction is still within the transition range at physiological temperature, is heterogeneous also in its affinities for specific receptor binding or other specific catabolic processes.

Acknowledgments

We wish to dedicate this article to Professor Anton Holasek, who has stimulated this investigation through many discussions, on the occasion of his 60th birthday. We are also indebted to Dr. G. Kostner for valuable advice, to Professors O. Kratky and J. Schurz for their support and interest in this work, and to Ulrike Rakusch and Doris Roblegg for excellent technical assistance.

References

Albers, J. J., Chen, C. H., & Aladjem, F. C. (1972) *Biochemistry 11*, 57.
Atkinson, D., Deckelbaum, R. J., Small, D. M., & Shipley, G. G. (1977) *Proc. Natl. Acad. Sci. U.S.A. 74*, 1042.
Bartlett, J. (1959) *J. Biol. Chem. 234*, 466.
Burstein, M., & Morfin, R. (1969) *Life Sci. 8*, 345.
Calvert, G. D., & Scott, P. J. (1975) *Atherosclerosis 22*, 583.
Deckelbaum, R. J., Shipley, G. G., Small, D. M., Lees, R. S., & George, P. K. (1975) *Science (Washington, D.C.) 190*, 392.
Deckelbaum, R. J., Shipley, G. G., & Small, D. M. (1977) *J. Biol. Chem. 252*, 744.
Eisenberg, S. (1976) *Atheroscler. Rev. 1*, 23.
Fidge, N. H., & Smith, G. D. (1975) *Artery 1*, 406.
Fisher, R. W. (1976) in *Low Density Lipoproteins* (Day, C. E., & Levy, R. S., Eds.) pp 151–195, Plenum, New York.
Fisher, R. W., Granade, M. E., Hammond, M., & Warmke, G. L. (1972) *Biochemistry 11*, 519.
Frings, C. S., Foster, L. B., & Cohen, P. S. (1971) *Clin. Chem. 17*, 111.
Glatter, O. (1977a) *J. Appl. Crystallogr. 10*, 415.
Glatter, O. (1977b) *Acta Phys. Austriaca 47*, 83.
Glatter, O. (1980) 5th International Conference on Small Angle Scattering, Berlin, Oct 1980, Abstract; (1981) *J. Appl. Crystallogr.* (in press).
Gofman, J. W., Rubin, L., McGinley, J. P., & Jones, H. B. (1954) *Am. J. Med. 17*, 514.
Goldstein, J. L., & Brown, M. S. (1977) *Annu. Rev. Biochem. 46*, 897.
Jackson, R. L., & Gotto, A. M., Jr. (1976) *Atheroscler. Rev. 1*, 1.
Jackson, R. L., Taunton, O. D., Segura, R., Gallagher, J. G., Hoff, H. F., & Gott, A. M. (1976) *Comp. Biochem. Physiol. 53B*, 245.
Janado, M., & Martin, W. G. (1968) *Can. J. Biochem. 46*, 875.
Janado, M., Martin, W. B., & Cook, W. H. (1966) *Can. J. Biochem. 44*, 1201.
Jürgens, G., & Kostner, G. M. (1975) *Immunogenetics 1*, 560.
Knipping, G. M. J., Kostner, G. M., & Holasek, A. (1975) *Biochim. Biophys. Acta 393*, 88.
Kostner, G. M. (1972) *Biochem. J. 130*, 913.
Kostner, G. M., & Holasek, A. (1972) *Biochemistry 11*, 1217.
Kratky, O. (1954) *Z. Elektrochem. 58*, 49.
Kratky, O. (1963) *Prog. Biophys. 13*, 105.
Kratky, O., Porod, G., & Kahovec, L. (1951) *Z. Elektrochem. Angew. Phys. Chem. 55*, 53.
Kratky, O., Porod, G., & Skala, Z. (1960) *Acta Phys. Austriaca 13*, 76.
Kratky, O., Leopold, H., & Stabinger, H. (1973) *Methods Enzymol. 27*, 98.
Laggner, P., & Stabinger, H. (1976) *Colloid Interface Sci. 5*, 91.
Laggner, P., & Kostner, G. M. (1978) *Eur. J. Biochem. 84*, 227.
Laggner, P., & Müller, K. (1978) *Q. Rev. Biophys. 11*, 371.
Laggner, P., Müller, K., Kratky, O., Kostner, G., & Holasek, A. (1976) *J. Colloid Interface Sci. 55*, 102.

Laggner, P., Degovics, G., Müller, K. W., Glatter, O., Kratky, O., Kostner, G., & Holasek, A. (1977) *Hoppe-Seyler's Z. Physiol. Chem. 358*, 771.
Lee, D. M. (1976) in *Low Density Lipoproteins* (Day, C. E., & Levy, R. S., Eds.) pp 3–47, Plenum, New York.
Lowry, N. J., Rosebrough, N. J., Farr, A. L., & Randall, R. J. (1951) *J. Biol. Chem. 193*, 265.
Luzzati, V., Tardieu, A., Mateu, L., & Stuhrmann, H. B. (1976) *J. Mol. Biol. 101*, 115.
Müller, K., Laggner, P., Glatter, O., & Kostner, G. (1978) *Eur. J. Biochem. 82*, 73.
Pownall, H. J., Shepherd, J., Mantulin, W. W., Sklar, L. A., & Gotto, A. M., Jr. (1980) *Atherosclerosis 36*, 299.
Stabinger, H., & Kratky, O. (1978) *Makromol. Chem. 179*, 1655.
Stabinger, H., & Kratky, O. (1979) *Makromol. Chem. 180*, 2995.
Stuhrmann, H. B., & Kirste, R. G. (1965) *Z. Phys. Chem. (Frankfurt am Main) 46*, 247.
Tall, A. R., Small, D. M., Atkinson, D., & Rudel, L. L. (1978) *J. Clin. Invest. 62*, 1354.
Tardieu, A., Mateu, L., Sardet, C., Luzzati, V., Aggerbeck, L., & Scanu, A. M. (1976) *J. Mol. Biol. 105*, 459.
Zipper, P. (1969) *Acta Phys. Austriaca 30*, 143.
Zipper, P. (1972) *Acta Phys. Austriaca 36*, 27.

Transbilayer Distribution of Phosphatidylethanolamine in Large and Small Unilamellar Vesicles†

J. R. Nordlund, C. F. Schmidt, S. N. Dicken, and T. E. Thompson*

ABSTRACT: There is much evidence which strongly suggests that most constituents of biological membranes display a transbilayer compositional asymmetry. The tendency of binary mixtures of phospholipids to form compositionally asymmetric bilayers spontaneously has been studied extensively. In small unilamellar vesicles, most mixtures of phospholipids with different head groups have been reported to be nonrandomly arranged across the bilayer. In this study, the influence of the radius of curvature on the transbilayer phospholipid distribution has been investigated. The distribution of egg phosphatidylethanolamine in large unilamellar vesicles comprised of egg phosphatidylethanolamine and egg phosphatidylcholine was determined by 2,4,6-trinitrobenzenesulfonic acid labeling. These large vesicles were obtained by modifying the ethanol injection procedure originally described by Batzri & Korn (1973) [Batzri, S., & Korn, E. D. (1973) *Biochim. Biophys. Acta 298*, 1015] by using a slow injection rate. After injection, the ethanol was removed by molecular sieve chromatography and the vesicle dispersion centrifuged. This results in a population of large, homogeneous, and unilamellar vesicles as determined by molecular sieve chromatography, ^{31}P NMR, and electron microscopy. The phosphatidylethanolamine component in unilamellar vesicles of this type is equally distributed between the two monolayers. In contrast, phosphatidylethanolamine in small unilamellar vesicles is known to be preferentially localized in the outer monolayer at low phosphatidylethanolamine concentrations and in the inner monolayer at high phosphatidylethanolamine concentrations. These results suggest that while phospholipids may form asymmetric bilayers spontaneously in highly curved regions of biological membranes, other factors must be responsible for the generalized phospholipid asymmetry seen in these systems.

It is generally believed that biological membranes are vectorial structures. Presumably, the different chemical environments and functional requirements found on opposing sides of the membrane dictate the arrangement of the membrane components. For example, all data indicate an absolute asymmetry in the orientation of membrane-bound proteins (Rothman & Lenard, 1977). Proteins that partially penetrate the membrane or are superficially attached to it are specifically located at one side while membrane-spanning proteins have well-defined orientations within the bilayer. Phospholipids are also distributed asymmetrically across the bilayer, although most phospholipids are present in both monolayers. The most convincing evidence for this has been obtained for erythrocytes. Data acquired by several techniques indicate that phosphatidylcholine and sphingomyelin occupy the outer monolayer whereas phosphatidylethanolamine, phosphatidylinositol, and phosphatidylserine are localized in the inner monolayer [reviewed by Op den Kamp (1979)].

Small unilamellar vesicles made by sonication (Huang, 1969) or rapid ethanol injection (Batzri & Korn, 1973) have been widely used as models for biological membranes. The highly curved surfaces characteristic of these vesicles are present in some specialized membrane structures such as the mitochondrial cristae or the microvilli of the intestinal epithelial cells. However, most biological membranes, like the plasma membrane or the delimiting membrane of cellular organelles, are essentially planar, although restricted regions may exhibit small radii of curvature (Thompson et al., 1974).

The utility of small unilamellar vesicles as model membranes must be assessed by their ability to approximate the biological structures they are expected to represent. Since the bilayers comprising these vesicles are highly curved whereas most biological membranes are not, it is important to explore the relationship between the radius of curvature and various bilayer properties. In fact, it has been shown that some physical properties of phospholipids, such as molecular motions (Sheetz & Chan, 1972) and the thermotropic behavior of the phospholipid components (Suurkuusk et al., 1976; Lentz et al., 1976a,b), are very sensitive to changes in the radius of cur-

† From the Department of Biochemistry, University of Virginia School of Medicine, Charlottesville, Virginia 22908. *Received November 26, 1980.* This investigation was supported by U.S. Public Health Service Grants GM-14628, GM-23573, and GM-17452.

0006-2960/81/0420-3237$01.25/0